Sensorless Temperature Estimation for Lithium-ion Batteries via Online Impedance Acquisition

Zheng, Yusheng; Weinreich, Nicolai André; Kulkarni, Abhijit; Sui, Xin; Teodorescu, Remus

Published in:
Energy Storage Conference 2023 (ESC 2023)

DOI (link to publication from Publisher):
10.1049/icp.2023.3103

Publication date:
2024

Sensorless Temperature Estimation for Lithium-ion Batteries via Online Impedance Acquisition

Yusheng Zheng[1], Nicolai André Weinreich[1], Abhijit Kulkarni[1], Xin Sui[1], Remus Teodorescu[1*]

[1]Department of Energy, Aalborg University, Aalborg, Denmark
**ret@energy.aau.dk*

Keywords: ENERGY STORAGE, BATTERIES, ELECTRIC VEHICLES, TEMPERATURE ESTIMATION, ELECTROCHEMICAL IMPEDANCE

Abstract

Temperature plays a significant role in the safety, performance, and lifespan of lithium-ion (Li-ion) batteries. To guarantee the safe, efficient, and long-lasting operations of batteries, one of the fundamental tasks of the battery management system (BMS) is to monitor battery temperature during operations. Nevertheless, subject to limited onboard temperature sensors, it becomes challenging for the BMS to obtain the temperature information of each cell in a battery system. To this end, this paper proposes a novel method to estimate the state of temperature (SOT) of batteries in real time based on the electrochemical impedance of batteries without the need for temperature sensors. By taking advantage of the smart battery architecture, the battery impedance at 5 Hz, which exhibit dependency on battery temperature while independency on the state of charge (SOC), can be obtained online via the bypass action. During battery operations, the impedance of the battery can be obtained through periodic bypass action and a designed filter. A simple impedance-temperature relationship that is calibrated offline, can be used to estimate and track the cell temperature. Experiments on charging show that the online calculated battery impedance has strong correlations to battery temperature, indicating its effectiveness in SOT estimation.

1 Introduction

Li-ion batteries nowadays are being widely applied to electric vehicles (EVs) and grid energy storage systems and have become a key enabling technology to reduce carbon emissions and facilitate sustainable energy development [1], [2], owing to their high energy/power density, high efficiency, and long cycle life [3], [4]. With the large-scale deployment of Li-ion batteries, the cells in the battery system need to be managed meticulously by the BMS in order to ensure safe, efficient, and reliable operations, where effective condition monitoring and active control are indispensable [5].

Temperature is one of the factors which has non-negligible impacts on many aspects of Li-ion batteries. For instance, when battery temperature exceeds the safety threshold under abuse conditions irrespective of the physical origin, battery failures such as thermal runaway will occur and cause catastrophic events [6]. At low temperatures such as 0 ℃, the available energy and power, as well as the charging acceptance of batteries decline dramatically, which brings range anxiety to many EV drivers and reduces the energy storage efficiency in the grid [7]. At both low and high temperatures, side reactions inside the battery associated with battery degradation become significant. For instance, the lithium plating and growth of the solid electrolyte layer (SEI) will cause accelerated battery aging [8]. Considering these negative effects of temperature on Li-ion batteries, the battery temperature needs to be regulated to an optimal range that is favorable to battery operations through the thermal management system. Therefore, one of the fundamental tasks of the BMS is to monitor battery temperature, which serves as the basis for active thermal management.

Nevertheless, in the state-of-the-art battery system, the number of temperature sensors is typically limited owing to the cost and complexity considerations. It is reported in the literature that the average sensor-to-cell ratio in nowadays battery systems is close to 1/10 [9]. Without the information of those sensor-free cells, it is difficult to achieve high-performance management of the battery system. For those cells without surface-mounted temperature sensors, their temperature information can only be estimated based on limited measurements such as current and voltage. As such, it is imperative to develop sensorless temperature estimation methods to obtain the temperature information of most cells in a battery system.

Generally, there are three types of methods to achieve sensorless temperature estimation, including impedance-based estimation, thermal model-based estimation, and data-driven estimation. Impedance-based estimation makes use of the relationship between the temperature and the electrochemical impedance of batteries, which can be calibrated offline by analyzing the electrochemical impedance spectroscopy (EIS) [10]. As for thermal model-based estimation, control-oriented thermal models which are able to trade off accuracy and low computational burdens need to be developed in the first place [11]. Then observers should be designed to estimate the battery temperature based on the current and voltage feedback [12], [13]. Data-driven estimation typically takes advantage of the nonlinear mapping capabilities of many machine learning algorithms such as neural networks to map the relationship between inputs (i.e., current and voltage) and the output such as the battery temperature in this case [14], [15]. Nevertheless, since the battery voltage is not sensitive to temperature, which brings difficulties to the design of the thermal model-based

SOT observer. In terms of data-driven estimations, the weak correlation between the input signal and battery temperature makes it difficult to develop an effective pure data-driven model [15]. Impedance-based estimation, on the other hand, can make use of the high sensitivity of battery impedance to temperature to estimate the SOT through a simple parameterized estimation function. It is simple and easy to implement in real-world applications, making it capable of being applied in BMS.

In this paper, we develop a novel method to estimate the battery temperature online via the temperature-dependent electrochemical impedance of Li-ion batteries. By analyzing the EIS of the battery under different SOCs and temperatures, a suitable frequency is selected under which the battery impedance is sensitive to temperature while insensitive to SOC. A smart battery architecture, which introduces switches to each cell, enables to bypass action of each cell with a certain frequency. The bypass action under the selected frequency can be performed periodically, and the impedance of the battery can be calculated online through the designed filters. Then the battery temperature can be estimated through an impedance-temperature relationship.

The remainder of this paper is organized as follows. Section 2 introduces the methodology for online impedance calculation. Section 3 presents the results of our method as well as the corresponding discussion. Then the main conclusion is provided in Section 4.

2. Methodology

2.1 Smart battery architecture with bypass

Traditionally, batteries in energy storage systems are not able to be controlled at the cell level. For instance, only the total current flowing through the battery pack can be controlled in conventional battery systems. However, the smart battery architecture, as illustrated in Fig. 1, enables the cell-level control of a battery system by introducing switches to each cell. The application of such power electronics to the energy storage system provides more control freedoms for the system. In this new architecture, a half-bridge circuit with MOSFETs is connected to each cell in a series-connected battery pack. A slave central processing unit (CPU) is allocated to each cell to control the two switches. In this way, the slave CPU can decide whether to bypass the cell or not [16].

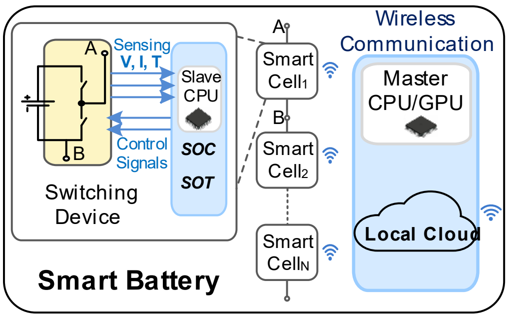

Fig. 1. The smart battery architecture [16].

Since the smart battery architecture enables the cell-level control of batteries, the bypass actions can bring new opportunities to the monitoring and control of battery cells in an energy storage system. With controlled bypass actions at certain frequencies, the pseudo-random sequence can be generated and the battery impedance can be obtained accordingly without the need for an external excitation source. In this way, the battery impedance at any desired frequency can be obtained in the context of smart battery architecture.

2.2 Frequency selection for online impedance acquisition

For impedance-based SOT estimations, the battery impedance needs to be measured online periodically during operations. Nevertheless, an EIS curve typically consists of the battery impedance from 0.01Hz - 10kHz, and measuring the impedance in that wide frequency range could be quite time-consuming, which makes the BMS unable to monitor battery SOT timely. Therefore, only the electrochemical impedance under certain frequencies can be measured to meet the demand of real-time SOT estimation.

In this paper, a frequency is selected based on the analysis of the EIS result under various SOCs and temperatures. Basically, the battery impedance (which denotes Z) depends not only on the excitation frequency f and temperature T, but also on the SOC. The impedance can be expressed as,

$$Z = g(f, T, SOC) \tag{1}$$

The battery impedance under the selected frequency f^* should be dependent on the cell temperature while insensitive to battery SOC to avoid the effect of SOC uncertainties on SOT estimation. In this regard, the battery impedance under f^* can be expressed as,

$$Z^* = g(T)|_{f=f^*} \tag{2}$$

2.3 Impedance Extraction

After selecting the suitable frequency for impedance-based SOT estimation, the online impedance calculation should be conducted in order to acquire the battery impedance via the bypass actions which are performed periodically throughout the battery operation. The impedance calculation framework is outlined in Fig. 2. The procedure takes the current signal during the bypass period and the corresponding voltage response as input and gives the calculated impedance magnitude as output for the specific target frequency. The main steps of the framework include upsampling, filtering, and amplitude extraction, which will be elucidated in this sub-section.

2.3.1 Upsampling

In cases where the sampling frequency is not high enough to capture the exact current and voltage waveform during the bypass action period, an upsampling step is required to artificially raise the sampling frequency for further processing. In this work, the current signal is a Constant Current (CC) charge signal interrupted by bypasses. Thus, a sample-and-hold strategy will help restore the analog current signal. However, limited prior knowledge about the voltage response makes it impossible to restore the signal without error. In prior testing, it was found that upsampling the voltage signal by sample and hold gave an adequate recreation of the analog voltage signal while avoiding complex upsampling strategies.

2.3.2 Filtering

Since the current and voltage signals during the bypass period may contain some components under other frequencies,

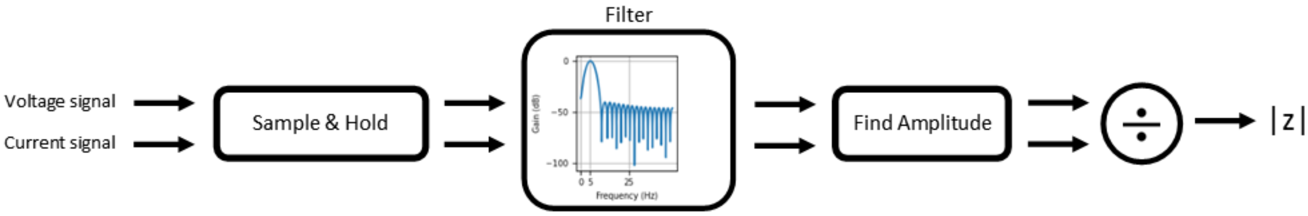

Fig. 2. Framework for the online impedance calculation during bypass action period.

these components are likely to interfere with the impedance extraction process. In our work, only the impedance at the selected frequency is needed for SOT estimation. Therefore, to avoid the influence of the unwanted signal components, filtering is used to extract the signals with target frequency from the previous upsampled signals. The filter should be designed to have 0 dB gain at the target frequency while attenuating all other frequencies. In addition, the filter should also be fast enough such that it converges during the bypass action period. To this end, a finite impulse response (FIR) band-pass filter is implemented with cut-off frequencies of 4 Hz and 6 Hz. The window method with 40th order Hamming window was used in the filter. It should be noted that prior to the filtering, the DC component of both signals was removed by subtracting their mean.

2.3.3 Amplitude Extraction & Impedance Calculation

The amplitudes of the filtered signals contain the impedance information of the battery cell under the selected frequency. In this work, the peak-to-peak amplitude was used to calculate the battery impedance during the bypass action period. Due to a large uniformity in the amplitude of both signals, the amplitude was extracted by subtracting the minimum signal value from the maximum. The impedance magnitude is then calculated by dividing the filtered voltage amplitude by the filtered current amplitude.

2.4 Online SOT estimation based on impedance calculations

Under the selected frequency, the relationship between the battery impedance and the temperature can be expressed in Eq. (2). The calculated impedance and the measured temperature under some operating conditions can be used for parameterizing the impedance-temperature relationship. Both the Arrhenius equation or 2nd order polynomial can be applied to fit the relationship between battery impedance and temperature. Then the estimation function can be constructed by performing the inverse function of Eq. (2) as,

$$\hat{T} = g^{-1}(Z^*) \qquad (3)$$

3 Results

In our work, a 3.7V/50Ah NMC Li-ion battery cell is studied by performing the EIS tests and CC charging tests with periodic bypass action. The experimental setup used in this study includes a battery tester, a thermal chamber, an electrochemical workstation, a temperature acquisition module, and a host computer. The EIS tests are performed in the first place at different ambient temperatures and SOCs through the electrochemical workstation to investigate the impedance characteristic of the battery. Then a suitable frequency is selected according to the EIS to perform the bypass actions. Instead of adding MOSFETs to the test cell, we merely use the pulse current in an on/off mode to simulate the bypass action via the battery tester during the CC charging tests, where the temperature is recorded by a temperature acquisition module. The results of the online impedance calculations and the subsequent impedance-based SOT estimations will be introduced in this section.

3.1 Frequency selection

The EIS results of the 50-Ah prismatic battery cell under different temperatures and SOCs can be shown in the Nyquist plot in Fig. 3. It can be seen from Fig. 3(a) that with the increase of battery temperature, the EIS shrinks significantly, particularly under low-frequency region, indicating the high sensitivity of the impedance to temperature. From Fig. 3(b) it can be concluded that the battery impedances at different SOCs start to converge when the frequency becomes higher. Unless the battery is operating at very low SOC (e.g., 10%), the effect of SOC on battery impedance is not as significant as the temperature does under the mid-high frequency region. Therefore, we select the 5 Hz as the bypass frequency, which is the maximum bypass frequency the battery tester can simulate.

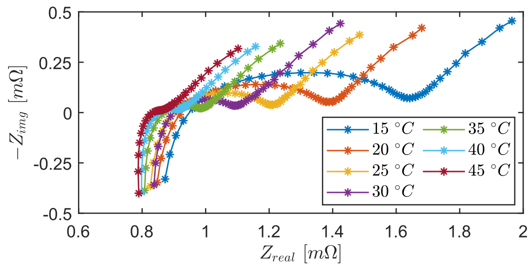

(a)

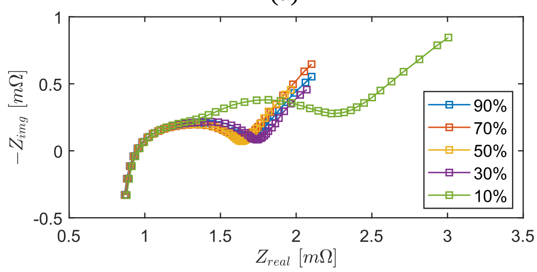

(b)

Fig. 3. EIS of the 50-Ah CALB battery under different temperatures and SOCs. (a) EIS at different temperatures when battery SOC is kept at 50%, (b) EIS at different SOCs when the battery temperature is kept at 25 ℃.

3.2 Impedance extraction

After selecting the bypass frequency, the bypass action is performed during the CC charging process. Take the 1C charging process as an example, as illustrated in Fig. 4. The bypass action takes place in the last 5 s of every half minute. When the cell is bypassed, the current flowing through the cell becomes 0, and while the cell is inserted the current is equal to the charging current.

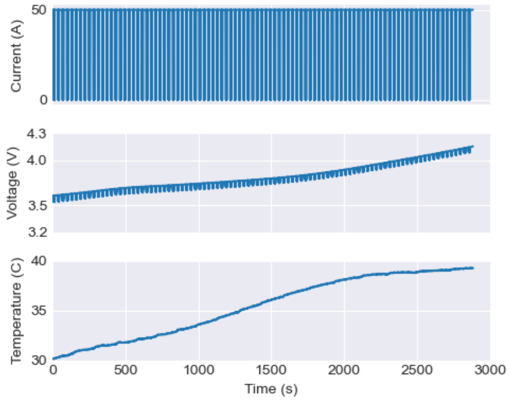

(a)

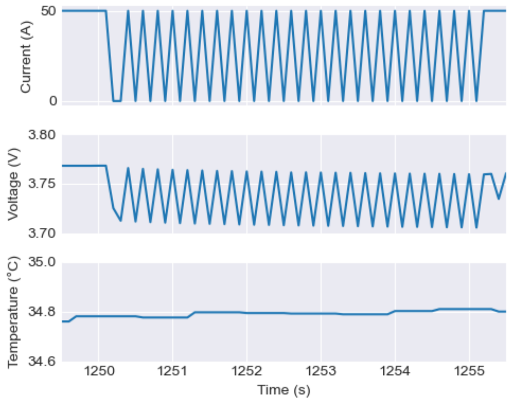

(b)

Fig. 4. Current, voltage, and temperature of the tested battery during 1C charging process with 5-s bypass actions every 30 seconds. (a) Measured data during the whole charging period. (b) Zoom of the measured data in one bypass action period.

Before the impedance calculation, both the current and voltage signals during the bypass period were upsampled by a factor of 10, giving a new sampling frequency of 95 Hz. Then these two signals are filtered via the designed band-pass filter, the result can be shown in Fig. 5. The filtered bypass signal becomes stable merely after 2 pulse cycles, indicating the effectiveness of the designed filter.

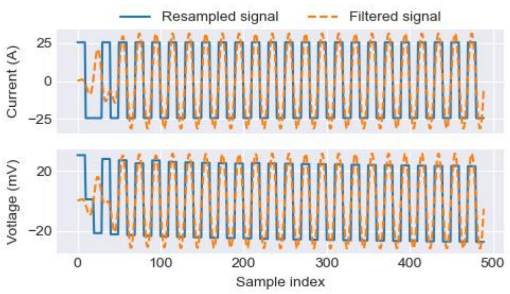

Fig. 5. Filtering result from the resampled current and voltage signals.

The relationship between the calculated impedance and the battery temperature during 1C charging can be illustrated as the solid blue dots in Fig. 6. The impedance-temperature relationship under 2C charging with 5-s bypass and 1C charging with 1-s bypass can also be shown in Fig. 6. Basically, the extracted impedance exhibits a nonlinear relationship with the battery temperature. As temperature increases, the impedance decreases. A 2nd order polynomial is used in our work to construct the estimation function based on the 1C charging scenario. Afterward, the battery temperature can be estimated via the estimation function, as shown in Fig. 7. Although the impedance-temperature relationship will vary with the operating conditions, future work can be conducted to develop an estimation function dependent on the current rate.

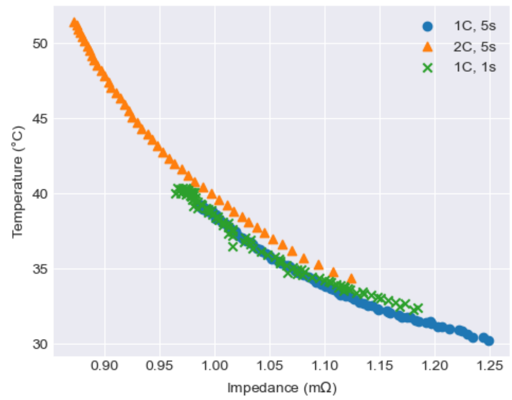

Fig. 6. Scatter plot of the Impedance vs. battery temperature under different charging rates and bypass periods.

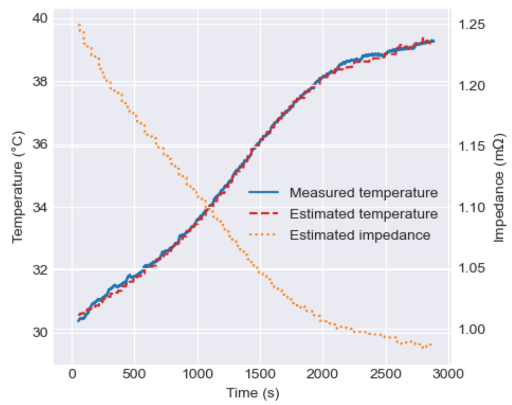

Fig. 7. Estimated battery temperature via the constructed impedance-temperature relationship and the online impedance measurement under 1C charging.

4 Conclusion

In this paper, we propose an online impedance measurement method to estimate the battery temperature in a sensorless manner, which is enabled by the smart battery architecture. Traditionally, battery impedance can only be measured under an equilibrium state using bulky impedance measurement instruments, or alternatively adding an extra excitation source to the battery system, which is not feasible in real-world applications if battery impedance needs to be measured online. The smart battery architecture allows the bypass action to be performed at a certain frequency so that the impedance can be extracted at the cell level online by processing the current and voltage signals during the bypass actions. In this way, the impedance measurement can be conducted when batteries are operating, without the need for any extra excitation source. We select 5 Hz to be the bypass frequency and propose a framework for online impedance calculation using the measured signals in the bypass period. This online impedance acquisition method has been applied to the CC charging process of batteries and a nonlinear relationship between the battery impedance and temperature can be observed. With the constructed estimation function, the battery temperature can be well estimated during the charging process. In addition, future work will focus on the implementation and validation of the proposed method in a real prototype.

5 Acknowledgements

This work was supported in part by the Villum Foundation for Smart Battery project (No. 222860).

6 References

[1] "BATTERIES| Towards a competitive European industrial battery value chain for stationary applications and e-mobility," 2020, Accessed: Jun. 24, 2022. [Online]. Available: https://www.era-learn.eu/documents/final_report_ms_partnerships.pdf

[2] "EV-Volumes - The Electric Vehicle World Sales Database." https://www.ev-volumes.com/ (accessed Mar. 06, 2023).

[3] J. B. Goodenough and K.-S. Park, "The Li-Ion Rechargeable Battery: A Perspective," J Am Chem Soc, vol. 135, no. 4, pp. 1167–1176, Jan. 2013, doi: 10.1021/ja3091438.

[4] R. Schmuch, R. Wagner, G. Hörpel, T. Placke, and M. Winter, "Performance and cost of materials for lithium-based rechargeable automotive batteries," Nature Energy, vol. 3, no. 4. Nature Publishing Group, pp. 267–278, Apr. 01, 2018. doi: 10.1038/s41560-018-0107-2.

[5] X. Hu, F. Feng, K. Liu, L. Zhang, J. Xie, and B. Liu, "State estimation for advanced battery management: Key challenges and future trends," Renewable and Sustainable Energy Reviews, vol. 114, p. 109334, Oct. 2019, doi: 10.1016/j.rser.2019.109334.

[6] T. M. Bandhauer, S. Garimella, and T. F. Fuller, "A Critical Review of Thermal Issues in Lithium-Ion Batteries," J Electrochem Soc, vol. 158, no. 3, p. R1, 2011, doi: 10.1149/1.3515880.

[7] X. Hu, Y. Zheng, D. A. Howey, H. Perez, A. Foley, and M. Pecht, "Battery warm-up methodologies at subzero temperatures for automotive applications: Recent advances and perspectives," Prog Energy Combust Sci, vol. 77, 2020, doi: 10.1016/j.pecs.2019.100806.

[8] J. S. Edge et al., "Lithium ion battery degradation: what you need to know," Physical Chemistry Chemical Physics, vol. 23, no. 14. pp. 8200–8221, 2021. doi: 10.1039/d1cp00359c.

[9] X. Lin, H. E. Perez, J. B. Siegel, and A. G. Stefanopoulou, "Robust estimation of battery system temperature distribution under sparse sensing and uncertainty," IEEE Transactions on Control Systems Technology, vol. 28, no. 3. pp. 753–765, 2020. doi: 10.1109/TCST.2019.2892019.

[10] H. P. G. J. Beelen, L. H. J. Raijmakers, M. C. F. Donkers, P. H. L. Notten, and H. J. Bergveld, "A comparison and accuracy analysis of impedance-based temperature estimation methods for Li-ion batteries," Appl Energy, vol. 175, pp. 128–140, 2016, doi: 10.1016/j.apenergy.2016.04.103.

[11] X. Hu, W. Liu, X. Lin, and Y. Xie, "A Comparative Study of Control-Oriented Thermal Models for Cylindrical Li-Ion Batteries," IEEE Transactions on Transportation Electrification, vol. 5, no. 4. pp. 1237–1253, 2019. doi: 10.1109/TTE.2019.2953606.

[12] M. Sajid, A. A. Hussein, A. Wadi, and M. F. Abdel-Hafez, "An Enhanced Fusion Algorithm With Empirical Thermoelectric Models for Sensorless Temperature Estimation of Li-ion Battery Cells," IEEE/ASME Transactions on Mechatronics, vol. 28, no. 2, pp. 621–631, Apr. 2023, doi: 10.1109/TMECH.2023.3235726.

[13] H. Pang, L. Guo, L. Wu, J. Jin, F. Zhang, and K. Liu, "A novel extended Kalman filter-based battery internal and surface temperature estimation based on an improved electro-thermal model," J Energy Storage, vol. 41, no. June, p. 102854, 2021, doi: 10.1016/j.est.2021.102854.

[14] Q. Yao, D. D. C. Lu, and G. Lei, "A Surface Temperature Estimation Method for Lithium-ion Battery Using Enhanced GRU-RNN," IEEE Transactions on Transportation Electrification, 2022, doi: 10.1109/TTE.2022.3197927.

[15] Y. Zheng, Y. Che, X. Hu, X. Sui, and R. Teodorescu, "Sensorless Temperature Monitoring of Lithium-ion Batteries by Integrating Physics with Machine Learning," IEEE Transactions on Transportation Electrification, pp. 1–1, 2023, doi: 10.1109/TTE.2023.3294417.

[16] R. Teodorescu, X. Sui, S. B. Vilsen, P. Bharadwaj, A. Kulkarni, and D.-I. Stroe, "Smart Battery Technology for Lifetime Improvement," Batteries, vol. 8, no. 10, p. 169, Oct. 2022, doi: 10.3390/batteries8100169.